Construction and Building Materials 419 (2024) 135481

Contents lists available at ScienceDirect

Construction and Building Materials

journal homepage: www.elsevier.com/locate/conbuildmat

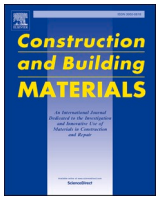

Evaluation of weathering resistance of cross-laminated timber blocks surface-treated with TiO_2 nanoparticles by liquid-precursor flame spray pyrolysis

Ganesh Sedhain [a], Yunsang Kim [a,*], Shuaib A. Mubarak [a], Thomas L. Eberhardt [b]

[a] Department of Sustainable Bioproducts, Mississippi State University, Starkville, MS 39759, USA
[b] USDA Forest Service, Forest Products Laboratory, Madison, WI 53726, USA

ARTICLE INFO

Keywords:
Wood modification
Titania coating
Flame spray pyrolysis
Superhydrophobic coating
UV protection
Accelerated weathering

ABSTRACT

Wood is a versatile and renewable resource utilized in a wide range of applications, including tools, furniture, construction, and advanced engineering structures. However, certain inherent properties of wood, such as moisture and ultraviolet (UV) degradation, impose limitations on its long-term durability and dimensional stability for outdoor applications. This research investigates the weathering durability of cross-laminated timber (CLT) blocks surface-treated with titanium dioxide (TiO_2) nanoparticles synthesized *via* liquid-precursor flame spray pyrolysis (FSP), directly deposited onto the surface of CLT blocks, and thereby resulting in a porous TiO_2 coating. This coating endows the CLT surface with superhydrophobic properties evidenced by a water contact angle of $\geq 150^{\circ}$. Results from scanning electron microscopy and X-ray diffraction show the coating to be comprised of crystalline, sub-100 nm individual and aggregated TiO_2 particles with significant porosity. Even after an 8-week accelerated weathering test, a portion of the crystalline TiO_2 particles remains on the CLT surface. The TiO_2-treated CLT demonstrates enhanced resistance to discoloration and gloss change over 8-weeks of accelerated weathering conditions, which are evidenced by a total color difference (ΔE) that is 3–4 times lower than that of the untreated CLT in the initial two weeks, and 58% lower after 8 weeks of weathering. Furthermore, the TiO_2-treated CLT exhibits fewer weathering defects, such as splits and cracks, than the untreated CLT. The enhanced weathering durability of the TiO_2-treated CLT is attributed to reduced lignin degradation, which is supported by the Fourier-transform infrared spectroscopy analysis. The findings of this study suggest that the TiO_2 coating by FSP offers a viable and cost-effective method for modifying engineered wood products for improving hydrophobicity and protecting against the deteriorating effects of UV irradiation and moisture exposure.

1. Introduction

Wood and wood-based products are well established as building and construction materials due to their appealing properties, including lightweight nature, high specific strength, low thermal expansion, and environmentally friendly and aesthetically pleasing attributes. Compared with other building materials such as steel, concrete, and masonry, wood is capable of sequestering carbon and has lower embodied energy, *i.e.*, the total energy used in the construction processes of a building, making a positive contribution to the building's carbon footprint. [1,2] However, one of the major drawbacks of wood is its outdoor degradation, typically described as weathering. Wood weathering leads to the deterioration of surface properties such as discoloration, heightened roughness, and the formation of cracks. Furthermore, weathering may cause changes in wettability, strength, and chemical compositions of wood, consequently diminishing its value as a building material. [3,4].

Weathering of wood is caused by photodegradation and photooxidative degradation of the wood cell wall polymers (cellulose, hemicelluloses, and lignin) and low molecular weight organic compounds known as extractives. When wood is exposed to natural light, which would penetrate wood up to ~200 μm, it generates free radicals that degrade lignin—an excellent UV absorber—and depolymerize the other organic components in wood. [5] It is important to note that due to the

* Corresponding author.
E-mail address: ysk13@msstate.edu (Y. Kim).

https://doi.org/10.1016/j.conbuildmat.2024.135481
Received 3 December 2023; Received in revised form 13 February 2024; Accepted 14 February 2024
Available online 27 February 2024

limited penetration depth of light, the weathering of wood is predominantly a surface phenomenon. There are numerous practices intended to mitigate the outdoor degradation of wood and wood-based products used as building materials. [6] These practices encompass surface treatments utilizing UV absorbers and radical scavengers, [7] solutions of inorganic metal compounds, [8] deposition of inorganic thin films, [9,10] and chemical grafting. [11] Treatments may also involve bulk modification of wood such as impregnation with thermosetting resins, [12] in-situ polymerization, [13] and thermal modification within the temperature range of 180–240 °C. [14] Among these approaches, there is an increasing focus on the use of nanomaterials to protect wood from outdoor weathering. [15] A promising strategy for enhancing the UV durability of wood and wood-based products involves incorporating metal oxide nanoparticles, such as TiO_2, ZnO, CeO_2, and Fe_2O_3, into clear exterior wood coatings. [6,8,16].

The application of inorganic nanoparticles onto the surface of wood can be achieved mainly by two methods: 1) the incorporation of the nanoparticles into conventional wood coating formulations, and 2) direct deposition of a thin film made of the nanoparticles onto wood surfaces. [6] The first method involves adding the nanoparticles, typically metal oxides as UV absorbers in colloidal form, to traditional wood coatings such as paints, varnishes, stains, and water repellents, which are commonly used to protect wood from outdoor weathering. Metal oxide nanoparticles are usually dispersed in the wood coating formulations, such as acrylic and polyurethane resins, which are subsequently applied onto wood surfaces by roller coating, brushing, or other applicators. [17–19] One advantage of incorporating nanosized metal oxides in the wood coatings is that the coatings remain clear, which would meet market expectations that rely on the intrinsic aesthetics of wood. However, the wood coatings incorporating metal oxide photostabilizers still lack durability and longevity, thereby restricting their use in outdoor woodwork unless regular maintenance is undertaken. [8].

Direct deposition of metal oxide nanoparticles onto the surface of wood allows for the formation of a thin film, resulting in an effective metal oxide coating on wood surfaces. For instance, several methods, including cold plasma spraying, [9,10] magnetron sputtering, [20] the sol-gel process, [21,22] and the hydrothermal process, [23,24] have demonstrated successful growth of ZnO, TiO_2, and CeO_2 films on the surface of wood. While certain wood substrates treated with metal oxides have shown improved durability against weathering, the practical implementation of such coatings on wood may not be feasible for commercial applications due to their complex nature, and the requirements for capital-intensive equipment and specialized process conditions.

Over the past two decades, there has been an increased interest in sustainable green building materials, which has led to extensive research in this field. As a result, the demand for wood has increased, prompting the development of innovative engineered wood products. Among these products, cross-laminated timber (CLT) has gained popularity due to its advantages over sawn timber, such as consistent strength and reduced variation across different products [2,25]. According to an international market report, the global CLT market is projected to reach $1.46 billion by 2024. [26] To further expand the use of CLT and compete with other building materials like concrete, steel, and masonry, certain challenges related to manufacturing standards, quality, and durability, need to be addressed. Additionally, CLT produced from wood is susceptible to degradation when exposed to UV radiation and moisture. When CLT panels are delivered to the construction site, they must be properly stored and adequately protected against weather elements. Wrapping or covering CLT panels with a tarpaulin is a standard practice in the construction industry for this purpose. However, contractors often fail to completely protect CLT panels on-site, resulting in some wood surfaces to become discolored or soiled during construction. [27] Therefore, protecting CLT from outdoor weathering, even if only temporarily, is crucial and requires comprehensive investigation. One effective approach to protect CLT from weathering by UV radiation and moisture can be the application of a TiO_2-based coating onto its surface.

The aim of this research is to examine weathering durability of CLT treated with TiO_2 nanoparticles by using liquid-precursor flame spray pyrolysis (FSP) against UV radiation and moisture under accelerated weathering conditions. FSP is a versatile technique capable of altering the surface properties of a wide range of materials, enhancing their resistance to wear, corrosion, and environmental factors. [28] In particular, the FSP process allows for the deposition of TiO_2 nanoparticles on cellulose-based heat-sensitive substrates such as paper and paperboard, improving their surface-wetting properties. [29,30] In this study, CLT samples treated with TiO_2 through FSP were subjected to accelerated weathering conditions for eight weeks. The surface morphology and wetting properties of the TiO_2-treated CLT were examined before and after the weathering, and the degree of discoloration and lignin degradation was investigated by using scanning electron microscopy (SEM) equipped with energy-dispersive X-ray spectroscopy (EDX), water contact angle (WCA), CIE $L^*a^*b^*$ color and gloss measurements, X-ray diffraction (XRD), and Fourier-transform infrared spectroscopy (FTIR).

2. MATERIALS AND METHODS

2.1. Sample preparation

CLT samples were cut from a larger three-ply CLT panel supplied by SmartLam, LLC (Whitefish, MT, USA) manufactured with Hem-fir. The size of the cut samples was 6.4 cm×6.4 cm×11 cm, selected as being suitable for the liquid-precursor FSP process and the accelerated weathering test, consisting of two outer layers having the same orientation and a perpendicular core layer. The longest sample dimension was that for the panel thickness, encompassing all three plies. A total of twenty-six samples, consisting of 10 samples as untreated CLT control, and 16 as TiO_2-treated CLT, were selected for the study based on the absence of any defects such as cracks, knots, resin pockets, and end joints. The face layer of each sample, a tangential surface, was sanded using a series of progressively finer grits of sandpapers from 100 to 3000 and cleaned with a brush. The sanded samples were then air-dried in an environmental chamber to a constant weight at 24 °C and a relative humidity of 66% until an equilibrium moisture content of 12% was achieved.

The air-dried samples were then subjected to the liquid-precursor FSP process, which deposited TiO_2 nanoparticles onto the top sanded surface of the 6.4 cm × 6.4 cm CLT. In liquid-precursor FSP, a liquid-phase precursor is sprayed through a pressure-assisted nozzle into a combustion source, a torch with propane gas as fuel in this study, turning the liquid precursor into vapor and subsequently into solid particles through pyrolysis. [28] A precursor solution consisting of 15 wt % titanium (IV) isopropoxide (TTIP) (>98% purity, Acros Organics) in isopropyl alcohol (IPA) was fed into an airbrush equipped with a 0.3 mm needle (Master airbrush model G22) operated by compressed air at a pressure of 8 – 10 psi (Master air compressor model TC-20). As shown in Fig. 1a, the angle between the airbrush and the propane torch was maintained at ~10°, while the distance between the airbrush and the CLT sample was set at 12.5 cm. [31] The CLT samples were mounted on a custom-made motorized stage operated by two stepper motors (DMX-JSA-17, Arcus Technology, USA), whose X and Y axis movement was programmed and controlled through a Windows graphical user interface. To ensure a uniform deposition of TiO_2 particles, the stage moved along a predetermined path at a speed of 1.5 cm/s that covered the entire surface of each mounted sample. Throughout the FSP process, the airbrush and the torch remained stationary (see Fig. 1b). A series of FSP deposition times of 5, 10, 20, and 30 minutes were employed to investigate the influence of this variable on weathering durability. Four replicate samples were prepared for each deposition time. The TiO_2-treated CLT samples were stored in the dark prior to the accelerated weathering test to minimize the photocatalytic activity of TiO_2.

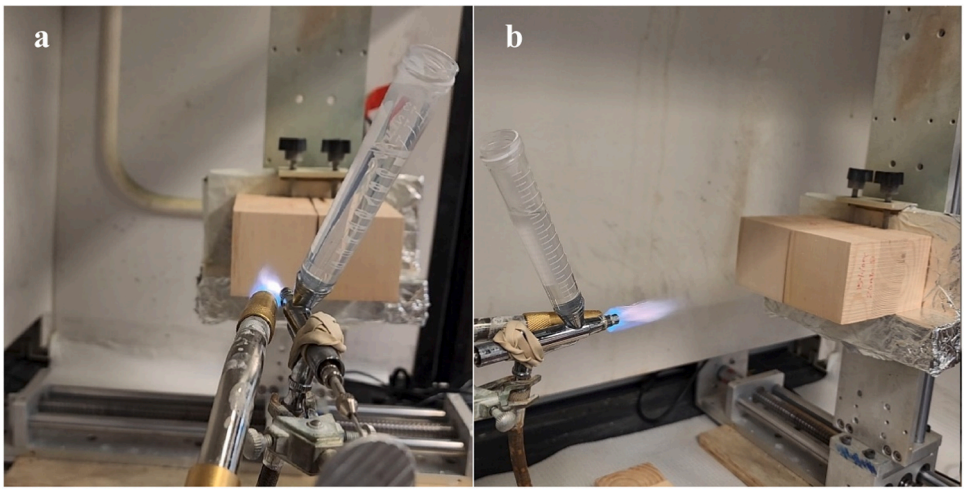

Fig. 1. . Photographs showing a liquid-precursor FSP process including a motorized stage.

2.2. Accelerated weathering test

Accelerated weathering testing was conducted using a custom-made weathering chamber that simulated UV radiation and moisture/rain conditions. The chamber was equipped with two 300 W UVA-340 lamps (OSRAM Vitalux) and a water spray. Following ASTM Standard G154–16, [32] the top surface of the CLT samples was exposed to an alternating cycle of 8-hour UV irradiance at 40 °C, followed by a 4-hour water spray at a rate of 0.36 liter/min for a total duration of 8 weeks. The layout of the samples in the weathering chamber is shown in Fig. 2.

2.3. Characterization: surface properties, crystallinity, and weathering degradation

WCA measurements were carried out by using the "drop-test plugin" available in ImageJ with a picture of a water droplet on the TiO_2-deposited CLT surface. A pipette was used to dispense a single droplet (about 3 – 5 μl) of deionized water on the coated surface. The picture of the droplet was taken after 2 s from a distance of 3 – 5 cm using the macro lens of a Samsung S22 ultra 1.0 smartphone. The surface morphology of the CLT samples before and after weathering was examined by SEM (JSM-6500 F, JEOL USA). Prior to imaging, thinly sliced CLT samples (1 – 1.5 mm) were mounted on an aluminum stub and sputter-coated with a 30 nm-thick layer of platinum. EDX elemental mapping was employed to compare the atomic weight percentage of carbon, oxygen, and titanium elements before and after the weathering exposure. To ensure the presentation of representative and unbiased SEM images for assessing changes to sample surfaces following FSP treatments and subsequent weathering, multiple slices were taken from at least two different CLT samples of the same kind. Images were captured at magnifications from 100x to 50,000x using at least two different spots sampled on each slice. The field of view for each image collected was carefully chosen in a way to accurately depict the average morphology of the respective sample. The images included were chosen considering focus, representativeness, and noise level. XRD spectra were obtained by a Rigaku Smartlab X-ray diffractometer equipped with Cu Kα radiation (λ = 1.54056 Å) over the 2θ range of 10 – 60° at a scan speed of 0.02°/min, to investigate the crystallinity of cellulose in wood and the TiO_2 particles deposited on CLT before and after the weathering exposure. Sample collection involved the use of a 1.5 mm thick wood slice for untreated CLT, while scraped particles were used for the TiO_2-treated CLT samples. FTIR was used to evaluate changes in the surface functional groups of wood after weathering. Thin surface slices of wood were collected with a razor blade from weathered samples and the reference without weathering. FTIR spectra were recorded using a Perkin-Elmer Spectrum Two spectrophotometer equipped with an attenuated total reflectance (ATR) accessory (single reflection diamond, Spectrum Two Universal ATR); spectra were collected over the range of 400–4000 cm^{-1} with a resolution of 4 cm^{-1} to determine the degradation of organic components in the wood.

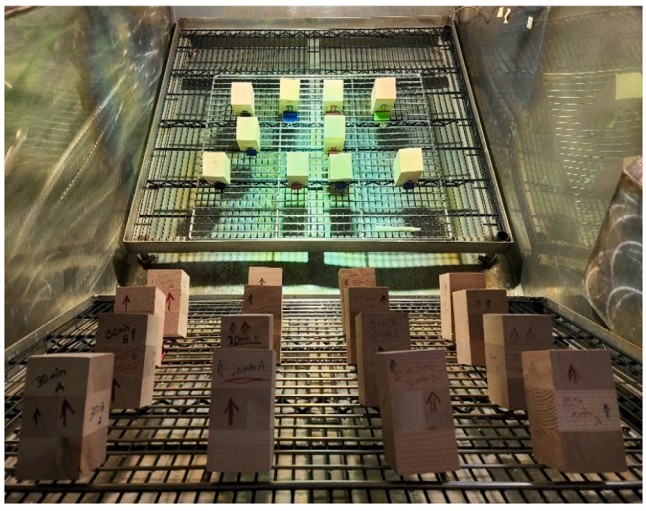

Fig. 2. An accelerated weathering chamber with CLT samples placed horizontally and on a holding platform at a 45° angle to UV bulbs.

2.4. Color and gloss measurements

The color parameters of the CLT samples were measured by using a handheld color spectrophotometer (CM-2300d, Konica Minolta, Osaka Japan). On a weekly basis, five readings were taken using the same spot during each measurement with a measurement diameter of 8 mm. The CIELAB 1976 color space was used to determine the discoloration of CLT samples. [33] This color system consists of three parameters, L^*, a^*, *and* b^*, which are three-dimensional representation of color as three values: L^* for luminance, and a^* and b^* for the color pairs of red/green and yellow/blue, respectively. The total color difference, ΔE, was calculated as a function of the accelerated weathering time according to the equation below,

$$\Delta E = \sqrt{\left(L_t^* - L_0^*\right)^2 + \left(a_t^* - a_0^*\right)^2 + \left(b_t^* - b_0^*\right)^2}$$

where L_0^* represents the luminance value before the weathering and L_t^*

denotes the luminance after a certain number of hours of weathering. A box plot was created by using OriginPro 2021, version 9.8.

The surface luster of CLT samples was measured by using a glossmeter (ETB-0686) following ISO 2813. [34,35] Three measurements were made on the same spot in the CLT sample used for the color measurement on a weekly basis. Readings were based on a specular gloss value of 96 gloss units (GU), scaled relatively to the perfect condition under identical illumination and view conditions of a highly polished, black glass standard with a defined refractive index of 1.567. To ensure consistent UV and moisture exposure conditions, the position of the CLT samples inside the weathering chamber was randomly rotated and mixed after each weekly measurement. The changes in color and gloss values were monitored to assess the weathering durability of the CLT samples.

3. RESULTS AND DISCUSSION

3.1. WCA

Table 1 shows the WCA of untreated and TiO_2-treated CLT samples as a function of FSP deposition time and storage days in the dark. Initially, the untreated control CLT sample exhibited a WCA of 83°, which significantly rose to >120° after the TiO_2 treatment by FSP. Upon storing the treated CLT samples in ambient darkness for 7 days, their WCAs reached a superhydrophobic threshold of ≥150°, while the WCA of the untreated CLT remained unchanged after the same period of storage in the dark. The increase in WCA remained consistent irrespective of the FSP deposition time (from 5 to 30 min). The enhanced hydrophobicity of the treated CLT can be attributed to a porous microstructure resulting from the deposition of TiO_2 particles on the wood surface, which will be further discussed in the SEM section below. The deposition of the nanosized particles on a surface not only augments its surface roughness, but also reduces the contact area between the surface and water droplets, thus promoting surface hydrophobicity. [36] Baxter and Cassie suggested that WCA increases as the contact area between a surface and water droplets decreases. [37] Superhydrophobicity of the TiO_2-treated CLT can be ascribed to the substitution of chemisorbed OH groups on the wood surface with oxygen from the air, as well as the accumulation of organic contaminants such as low-molecular-weight hydrocarbons. [38–41] The increase in WCA was initially rapid in the first few days of dark storage, which saturated as the WCA approached the superhydrophobic threshold. No significant further increase in WCA for the treated CLT samples was observed after 7 days of storage in the dark.

The WCA of both untreated and treated CLT samples decreased significantly following the weathering test, regardless of the duration of FSP deposition time. Specifically, the 8-week accelerated weathering turned all untreated and treated CLT samples into superhydrophilic surfaces (WCA ~0°), causing the rapid penetration of water droplets into the wood surface. Similar findings have been reported in previous studies, in which untreated and TiO_2-coated wood surfaces exhibited a decline in WCA after exposure to UV radiation and water spray for 960 hours. [42] This change in wettability can be attributed to the impact of UV exposure on the weathering of wood surfaces, which is often associated with discoloration, cracking, as well as changes in wood properties such as surface roughness, strength, wettability, and chemical changes of the organic components in wood. [3,43] The reduction in WCA observed in the TiO_2-treated CLT samples may also be associated with a morphological change in the TiO_2 particles on the CLT surface following the weathering test, as further discussed in the SEM section below.

Table 1
WCA of untreated and TiO_2-treated CLT samples as a function of FSP deposition time and days stored in the dark.

Days in dark storage	Untreated CLT	TiO_2-CLT, 5-min FSP	TiO_2-CLT, 10-min FSP	TiO_2-CLT, 20-min FSP	TiO_2-CLT, 30-min FSP
1	83°	121°	125°	121°	122°
3	83°	133°	139°	134°	n/a
7	83°	150°	150°	150°	151°

3.2. SEM and EDX

Top-surface SEM images of the untreated (Fig. 3a) and TiO_2-treated CLT samples (Fig. 4a, b, e, and f) show that the FSP process successfully deposited TiO_2 particles on the wood surface, creating a coating-like morphology. Regardless of the deposition time, there were fine sub-100 nm TiO_2 particles deposited on the surface along with some aggregates, which is a natural nanoparticle phenomenon, making distinguishing individual particles from aggregates difficult. SEM images at higher magnification (Fig. 4b and f) show that the sub-100 nm TiO_2 particles created a highly porous morphology effectively covering a large surface area. A seemingly thicker and denser TiO_2 layer was observed for 20-min FSP sample than 10-min FSP. Several studies reported a similar porous structure for TiO_2 coating on a wood surface by plasma, hydrothermal, and solvothermal treatments. [24,44,45].

Comparing the SEM images for control samples before (Fig. 3a) and after weathering (Fig. 3b), the formation of several cracks and voids on the surface was observed after weathering the samples. These defects can be related to the weakening of the cell walls and the development of longitudinal macro- and micro-cracks in the weathered cell wall, resulting from the degradation of wood components such as lignin. [39] The SEM images of the TiO_2-treated CLT samples in Fig. 4c, d, g, and h reveal that some TiO_2 particles were present on the sample surface even after 8 weeks of accelerated weathering, which will be further discussed in the context of the EDX analysis. However, the porous microstructure of the TiO_2 layer was observed to be changed. In particular, SEM images at higher magnification for TiO_2-CLT after weathering (Fig. 4d and h) show the microstructure to be significantly less porous with dense and aggregated clusters of TiO_2 particles. This change could result from some TiO_2 particles being stripped and/or washed away during the weathering process and possibly be related to the decrease in wettability properties due to the changes in the microstructure and roughness of the wood.

Fig. 5 shows SEM images of untreated and treated CLT samples before and after weathering along with the corresponding EDX mapping and spectra with atomic mass percentages thereof. The EDX mapping and spectra of titanium (Ti) associated with the TiO_2-treated CLT samples (Figure 5c4 – c5, d4 – d5, e4 – e5, and f4 – f5) further confirm the presence of TiO_2 particles and their uniform distribution on the wood. An identical trend was observed for the treated CLT samples, both before and after the accelerated weathering test, as observed in the SEM images of Fig. 4 and Fig. 5. Notably, the atomic% of titanium increased with the FSP deposition time, corroborating the presence of the denser and thicker TiO_2 layer observed in the 20-min FSP sample compared to the 10-min sample, which is clearly seen in the SEM images in Figs. 4a – b and 4e – f. After weathering, all the samples exhibited a decrease in the atomic% of carbon accompanied by an increase in the atomic% of oxygen, indicating the occurrence of oxidation that seemed to be consistent regardless of the TiO_2 treatment. The atomic% of titanium for the TiO_2-treated samples was expected to decrease after weathering, which was observed only in the 20-min FSP sample. Weathering of wood would lead to the formation of micro- and macro-cracks, making it challenging to perform a quantitative analysis of the atomic% of titanium using EDX data.

3.2.1. XRD

Fig. 6 exhibits the XRD data for untreated and TiO_2-treated CLT samples before and after the accelerated weathering test. The untreated CLT showed the peaks at $2\theta = 15–16.5°$, 22.3 – 22.4°, and 32.3 – 34.3°,

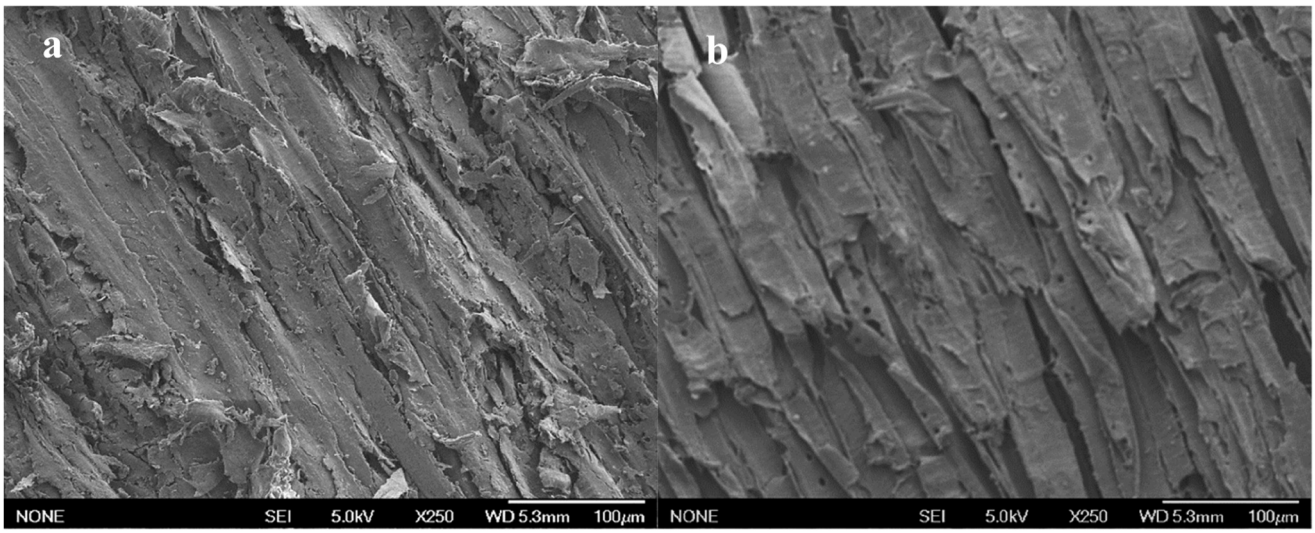

Fig. 3. . SEM images of untreated CLT samples: (a) before and (b) after accelerated weathering test.

which are assigned to the crystalline planes of (101) and (10$\bar{1}$), (002), as well as (004) from the typical cellulose I structure in wood according to JCPDS data 03–0289. [46] The position, intensity, and overall shape of these peaks remained the same regardless of the weathering. TiO_2--treated CLT samples before the weathering test showed characteristic peaks for the anatase phase in TiO_2 at $2\theta = 25.35°$, 37.9°, and 48.1° corresponding to the crystalline planes of (101), (004), and (200). In comparison, the peaks for the rutile phase were observed at $2\theta = 27.5°$, 36.2°, 41.3°, and 54.4° corresponding to the crystalline plane of (110), (101), (111), and (211). All the peaks were identical to the standard spectra to JCPDS data 88–1175 and 84–1286. This supports the successful deposition of crystalline TiO_2 particles on the surface of CLT. After the weathering test, these characteristic peaks corresponding to the anatase and rutile phases were still present in TiO_2-CLT with reduced intensity. Notably, TiO_2-CLT samples after weathering in Fig. 6b contained peaks attributed to cellulose crystals, suggesting the sample collection method involving surface scraping of TiO_2-CLT after weathering included a significantly higher proportion of wood compared to TiO_2-CLT before weathering. It is probable that weathering contributed to the removal and erosion of some TiO_2 particles from the surface of wood. Nevertheless, the XRD spectra of TiO_2-CLT after weathering indicate that the deposited TiO_2 on CLT retained its original crystalline structure after the weathering test.

3.3. Color and gloss before and after weathering

Fig. 7 shows the photographic images of untreated and TiO_2-treated CLT samples with varying FSP deposition time (5 – 30 minutes) under the weathering exposure period of up to 8 weeks. The untreated sample shown in the top row in Fig. 7 exhibited rapid discoloration within the first week, leading to substantial darkening. This discoloration can be linked with lignin degradation on the surface of wood, leading to the formation of chromophoric substances such as carboxyl and carbonyl groups. Additionally, the discoloration is believed to be related to extractives moving from the inside to the surface of wood. [5,7,47] As the weathering went on from week 2–8, the darkening appeared to gradually diminish, resulting in a somewhat whitish hue in the untreated sample. It is known that the prolonged duration of weathering increases the likelihood of not only chromophoric substances leaching away with water, but also the extractives undergoing further degradation. This process would result in a whitish surface appearance on wood, characterized by a higher concentration of cellulose and hemicellulose. [48].

When examining TiO_2-treated CLT samples with the FSP deposition time of up to 30 min, we observed significantly reduced initial discoloration and associated darkening during the first week compared to the untreated CLT. Except for the 5 and 10 min TiO_2-treated samples, the discoloration within the first week of weathering was so marginal that it was hardly even distinguishable from the photographs presented in Fig. 7. Given that TiO_2 is a well-known UV absorber that will reduce photo-induced degradation of lignin and extractives in wood, we believe that the TiO_2 treatment on CLT created a protective layer, thereby enhancing the weathering durability of CLT. [42,49–51] Notably, cracking was less pronounced in the TiO_2-treated samples compared to the untreated one, indicating an overall improvement in weathering durability after the TiO_2 treatment.

Figs. 8a – 8d shows the color parameters (L^*, a^*, and b^*) and gloss values for the untreated and TiO_2-treated CLT samples during the accelerated weathering test up to 56 days (8 weeks). Ten individual samples for the untreated CLT and four individual samples for the TiO_2-CLT with 5, 10, 20, and 30 minutes of FSP deposition times were measured. An individual data point represents each week's average measurement from 0 (before weathering) to 8 weeks.

The untreated CLT samples showed a substantial darkening with an 18% reduction in L^* during the first week (Fig. 8a). In contrast, a^* and b^* increased by 28% and 27%, respectively, indicating a color shift towards reddish and yellowish hues (Figs. 8b and 8c). However, these initial changes in L^*, a^*, and b^* were rapidly subdued as weathering continued. Specifically, L^* gradually rose from 62.4 after the first week to 66.3 after eight weeks, while a^* and b^* kept decreasing after week 1. The gloss value also followed a similar trend to L^*. This trend aligns with the discoloration of the untreated CLT sample shown in Fig. 7, in which the rapid darkening and an increase in yellowness in the first week were followed by a more gradual color change in the subsequent weeks.

The TiO_2-treated CLT samples exhibited a comparable pattern in L^*, a^*, b^*, and gloss to the untreated CLT with considerably subdued values in all these parameters. We note that before weathering the TiO_2-CLT exhibited higher L^* and lower a^*, b^*, and gloss when compared to the untreated CLT, probably due to the reflection and/or scattering of light by the deposited TiO_2 nanoparticles. During the first week, the reduction in L^* for the TiO_2-CLT was 8.1%, 8.4%, 5.8%, and 6.8% for 5, 10, 20, and 30 min FSP samples, respectively, which was more than twice as low as the initial L^* reduction for the untreated CLT. The reduced initial darkening of the TiO_2-CLT suggests the TiO_2 treatment effectively mitigated the degradation of lignin and low-molecular-weight extractives. The decrease in L^* continued until week 8 for all TiO_2-CLT, while the untreated CLT ceased to decrease after week 3, and its values started to rise. Notably, the untreated CLT exhibited a 9.1% increase in L^* between weeks 3 and 8, which may result from a gradual reduction of the

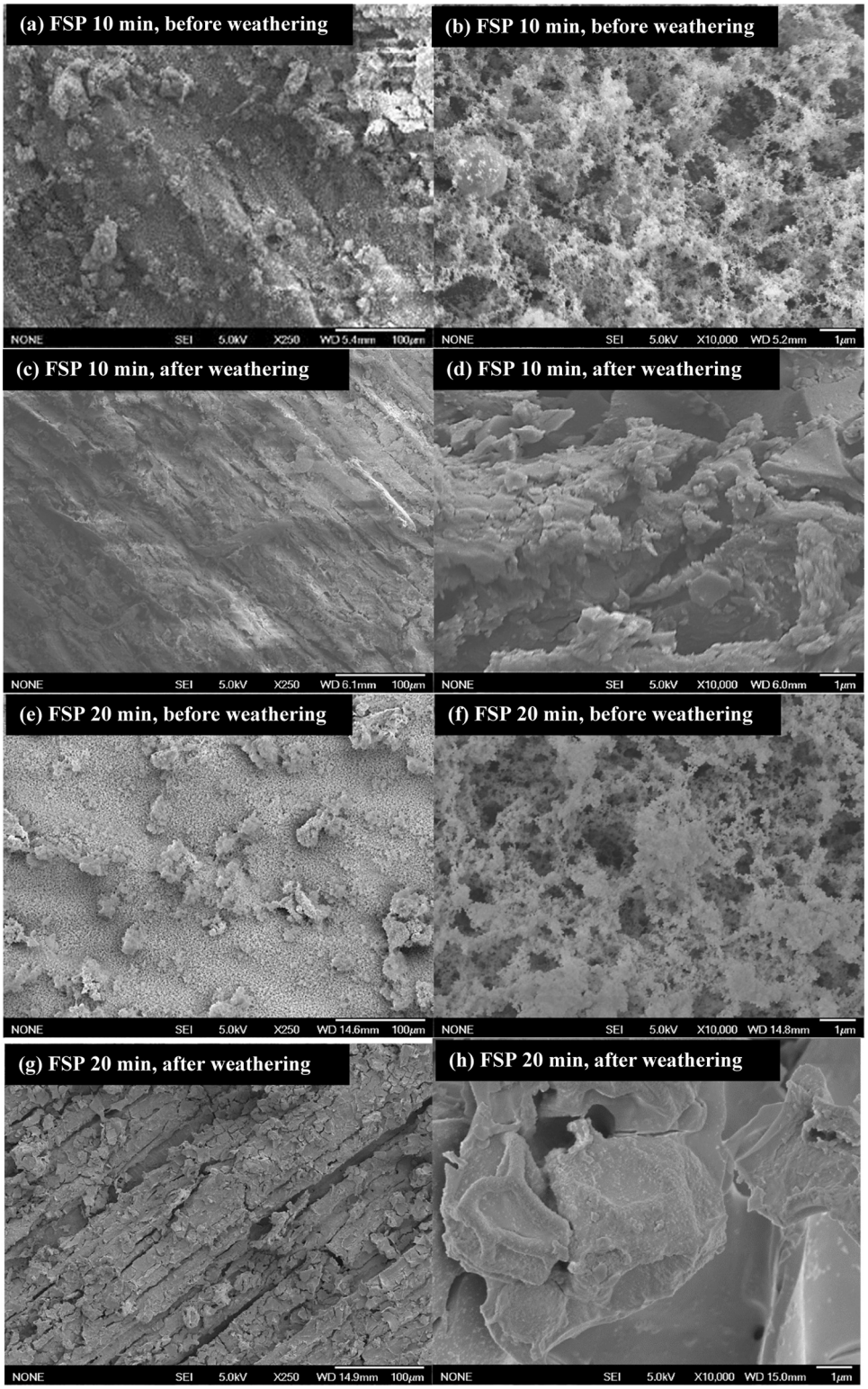

Fig. 4. SEM images of TiO_2-treated CLT samples: (a, b, e, f) before and (c, d, g, h) after accelerated weathering test.

chromophoric compounds on the CLT surface, as well as further degradation of extractives that would leave a whitish hue. [48] In contrast, all TiO_2-CLT showed only a marginal decrease in L^*, less than 2.8%, during the same period, suggesting that the TiO_2 treatment provided extended protection against darkening from UV exposure of accelerated weathering. It is worth noting that the standard deviation in L^* was most pronounced for 5 min FSP among the TiO_2-CLT samples. We believe a longer FSP time resulted in a more uniform deposition of TiO_2 nanoparticles, contributing to overall reduced fluctuation in L^*. After week 8, L^* values appeared to converge for all samples, regardless of the TiO_2 treatment and the FSP time.

Similar to L^*, the values of b^* and gloss for the TiO_2-CLT exhibited a substantial reduction in their initial changes after the first week compared to the untreated CLT. Subsequently, they gradually

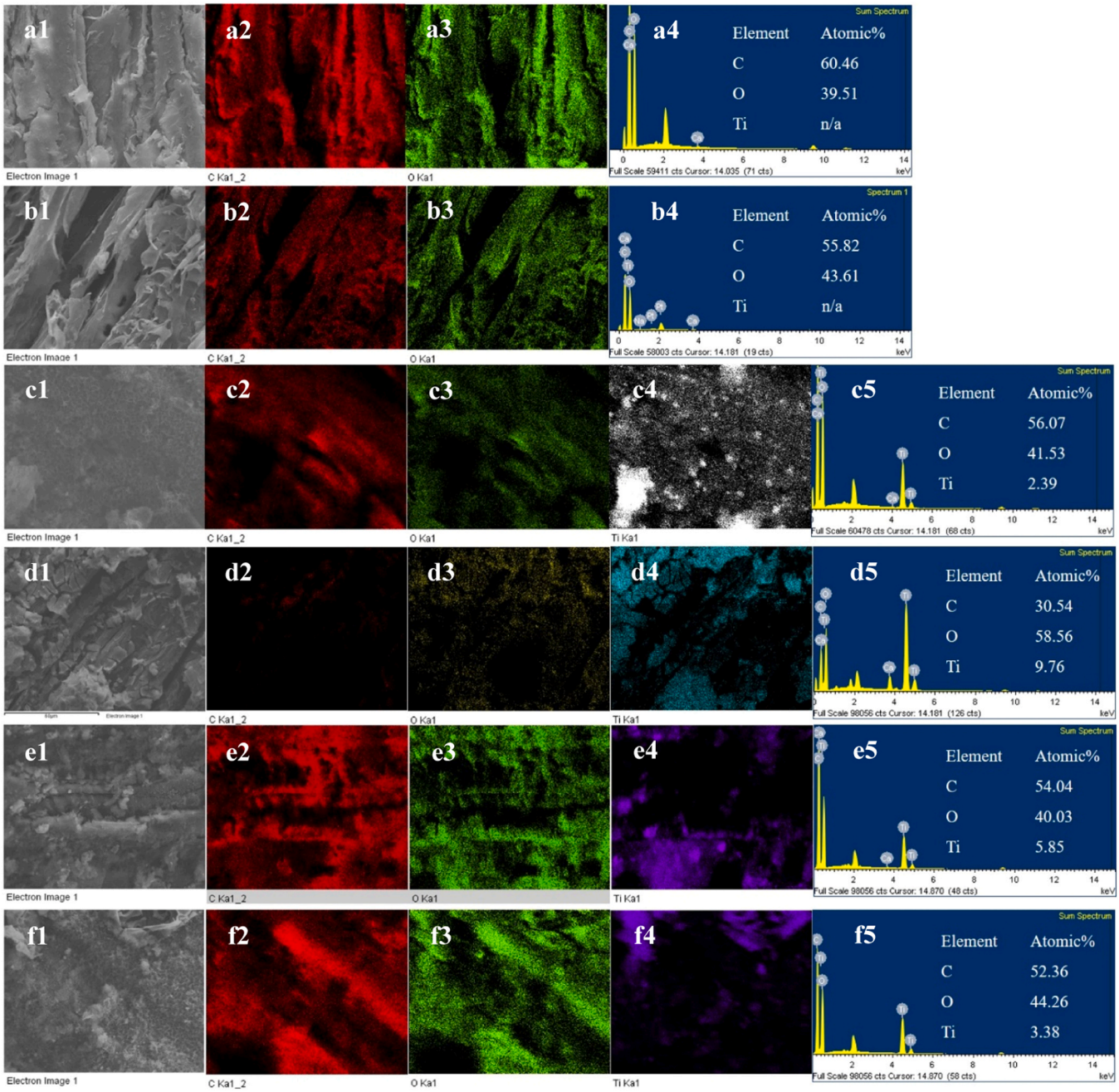

Fig. 5. SEM images of untreated CLT (a1) before and (b1) after weathering and the corresponding EDX mapping of: (a2, b2) carbon, (a3, b3) oxygen, and (a4, b4) EDX spectra with atomic mass percentages. SEM images of 10-min FSP TiO_2-treated CLT (c1) before and (d1) after weathering and the corresponding EDX mapping of: (c2, d2) carbon, (c3, d3) oxygen, (c4, d4) titanium, and (c5, d5) EDX spectra with atomic mass percentages. SEM images of 20-min FSP TiO_2-treated CLT (e1) before and (f1) after weathering and the corresponding EDX mapping of: (e2, f2) carbon, (e3, f3) oxygen, (e4, f4) titanium, and (e5, f5) EDX spectra with atomic mass percentages.

approached values similar to those of the untreated CLT by week 8. It is worth mentioning that the gloss values for the TiO_2-CLT remained much lower than that of the untreated CLT. Within the first week, the untreated CLT showed a 26.8% increase in b^* and a 36.7% reduction in gloss, whereas the TiO_2-CLT showed only up to a 14.0% increase in b^* and up to a 16.8% reduction in gloss during the same period. Although the a^* values were consistently lower in the TiO_2-CLT than the untreated CLT, the relative change in a^* remained similar between the untreated and TiO_2-treated CLT samples.

During the photo-induced discoloration of wood, luminance, L^*, generally undergoes more significant changes than the chromaticity indices, a^* and b^*, [52] which is also evident in the $L^*a^*b^*$ changes illustrated in Figs. 8a – 8c in our study. Thus, a change in L^* tends to correlate strongly with the total color difference, ΔE.

Fig. 8e shows ΔE of the untreated and TiO_2-treated CLT samples over the course of 8 weeks of accelerated weathering. The untreated CLT exhibited a high ΔE of up to 20 during week 1 and 2, indicating intensive early discoloration. Given that $\Delta E \approx 2.3$ corresponds to a just noticeable difference (JND), [53] in which an observer can detect a color difference with the naked eye only after a certain threshold of JND, the early discoloration of the untreated CLT was extensive. As weathering continued, ΔE gradually reduced to 12 by the end of week 8. In contrast, the TiO_2-CLT showed ΔE values that were 3–4 times lower than the untreated CLT in week 1 and 2, demonstrating superior weathering

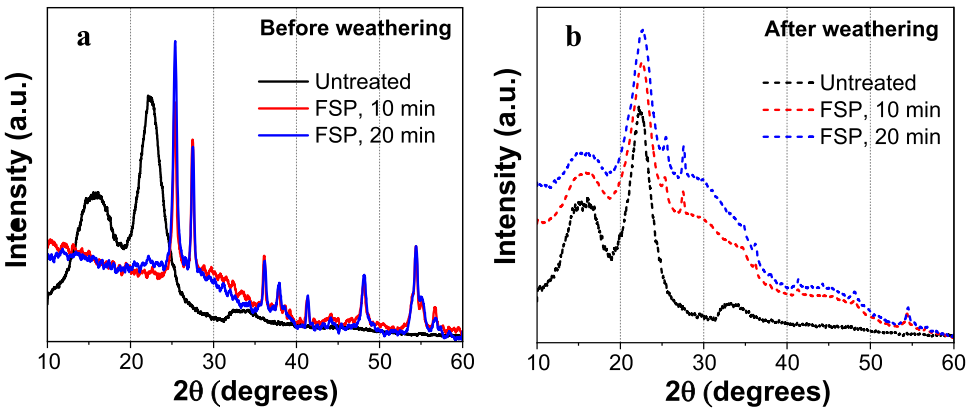

Fig. 6. XRD spectra for untreated and TiO_2-treated CLT samples (10 and 20 min FSP deposition times): (a) before and (b) after the accelerated weathering test.

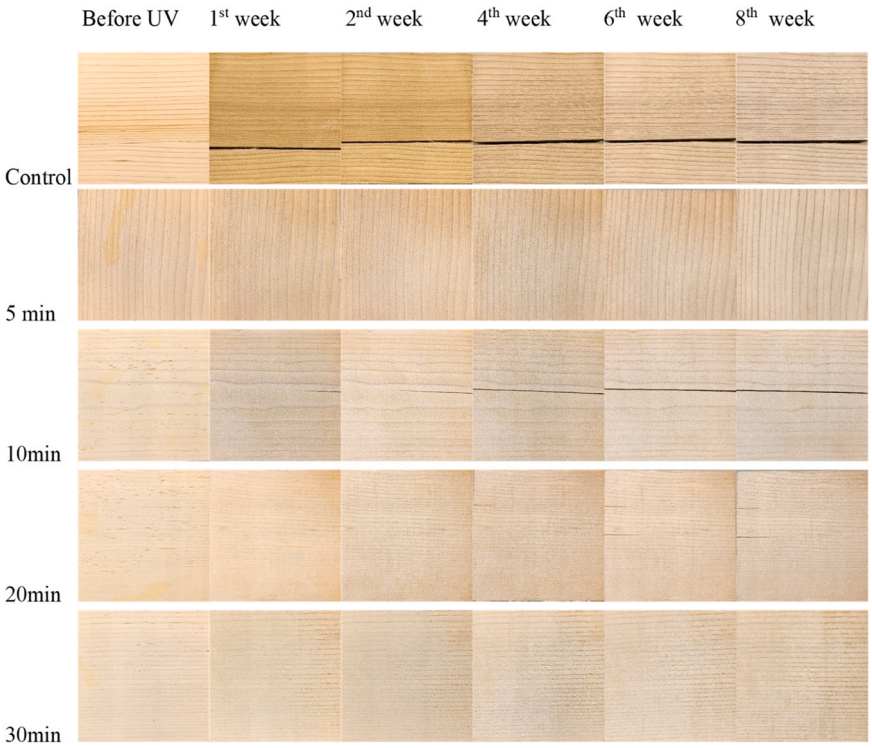

Fig. 7. Photographs of untreated and TiO_2-treated CLT samples (5 – 30 min of FSP deposition) over an accelerated weathering period of up to 8 weeks.

performance, particularly in terms of early discoloration. We also note that ΔE values of the TiO_2-CLT were lower with reduced fluctuations when subjected to the FSP process lasting longer than 5 minutes, as evidenced by the substantially narrower 2 interquartile ranges (2IQR) observed for TiO_2-CLT samples at 10, 20, and 30 min FSP treatments (Fig. 8f), which suggests the FSP process exceeding five minutes is desirable. As weathering continued, the difference in ΔE between the untreated and TiO_2-treated CLT gradually diminished. Nonetheless, by the end of week 8, the ΔE values of the TiO_2-CLT remained considerably lower than that of the untreated CLT. Specifically, ΔE for the TiO_2-CLT, 20 min FSP after week 8 was 7.8, which was 58% lower than ΔE of the untreated CLT. Since ΔE values appeared to stabilize around week 6 or 7 for both the untreated and TiO_2-treated CLT samples, we anticipate that the TiO_2-CLT would potentially exhibit superior long-term discoloration resistance compared to the untreated CLT, which deserves further investigation. In terms of the total color difference up to 8 weeks of accelerated weathering, the TiO_2-CLT with 20 min FSP performed the best, given its median and mean ΔE values as well as its reduced statistical dispersion illustrated in Fig. 8f.

3.4. FTIR spectroscopy

The chemical changes in the surface of untreated and TiO_2-treated CLT samples after weathering were evaluated by FTIR in Fig. 9. The impact of weathering was assessed by using the transmittance ratio, I_{lig}/I_{carb}, representing lignin and carbohydrate (polysaccharide) components in wood. Specifically, the quantification of lignin degradation by weathering was based on the C=C stretching of the aromatic ring in lignin at 1510 cm^{-1} and the C-H symmetric deformation in polysaccharides at 1375 cm^{-1}. [19,54–57] These peaks were chosen due to their relevance in reflecting the photodegradation mechanism of the organic components in wood. Lignin, which is a strong UV absorber, undergoes degradation during weathering while cellulose remains relatively unaffected. In Fig. 9, the FTIR spectra for TiO_2-treated samples showed that the shape and intensity of the lignin band at 1510 cm^{-1} remained unchanged after weathering, while those of the untreated

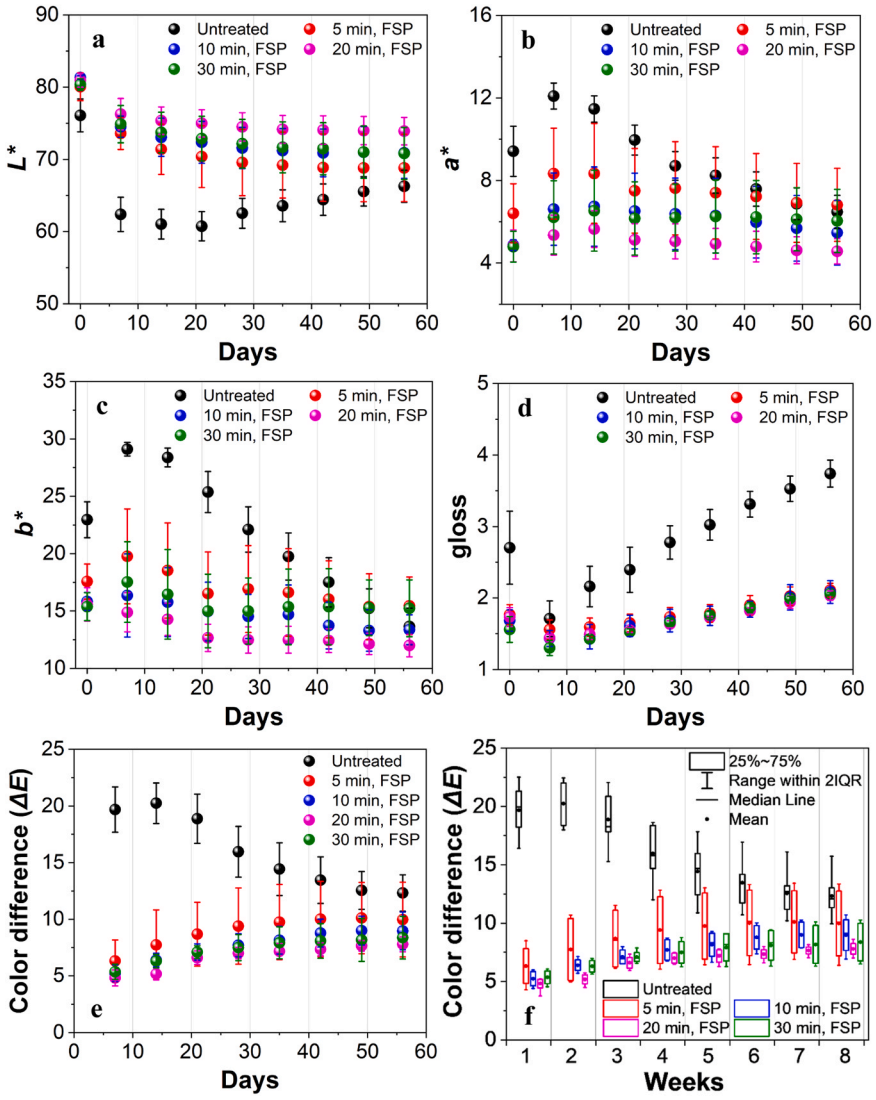

Fig. 8. CIELAB color and gloss values for the untreated and TiO_2-treated CLT samples (5 – 30 min of FSP deposition) during the accelerated weathering test up to 56 days (8 weeks): (a) L^*, (b) a^*, (c) b^*, (d) gloss, and (e) the total color difference, ΔE. (f) A box plot illustrating the statistical population of ΔE, including boxes representing the 25th and 75th percentiles, whiskers indicating 2 interquartile ranges (2IQR), along with median and mean values, for the untreated and TiO_2-treated CLT samples across the 8-week accelerated weathering test.

sample were significantly affected and reduced. Conversely, the carbohydrate band at 1375 cm^{-1} for both untreated and TiO_2-treated samples seemed unaffected by weathering. Indeed, the transmittance ratio, $I_{li\text{-}g}/I_{carb}$, exhibited only marginal changes for the TiO_2-treated samples after weathering, while the untreated sample showed a pronounced increase due to lignin degradation. The unchanged transmittance ratio for TiO_2-CLT suggests that the TiO_2 treatment by FSP mitigated and reduced the photodegradation of lignin in wood.

4. Conclusions

We demonstrate the enhanced weathering durability of CLT through a surface treatment with TiO_2 nanoparticles, which were directly deposited onto CLT by using liquid-precursor flame spray pyrolysis (FSP). The TiO_2 treatment on CLT blocks was performed under ambient conditions, after which the CLT samples were subjected to accelerated weathering for eight weeks. The FSP treatment on CLT rendered a porous, superhydrophobic layer consisting of crystalline, sub-100 nm TiO_2 particles. TiO_2-treated CLT exhibited significantly less discoloration than untreated CLT, in which the total color difference, ΔE, of TiO_2-treated CLT was found to be up to 58% lower than that of the untreated CLT after 8 weeks of weathering. Improved weathering durability of TiO_2-treated CLT is attributed to reduced lignin degradation. The collective results suggest the TiO_2 coating by FSP holds promise in enhancing the properties of engineered wood products and potentially extending their outdoor service life. Considering its portable and low resource-requirement nature, the FSP process has practical appeal beyond the CLT industry, potentially for providing temporary on-site protection of other types of wood-based products such as structural timbers. Building upon this initial investigation, further efforts will be made to integrate the TiO_2 coating by FSP with a binder system that will aim to enhance longevity and durability.

CRediT authorship contribution statement

Eberhardt Thomas L.: Writing – review & editing, Supervision, Resources, Project administration, Funding acquisition. **Mubarak Shuaib Ahmed:** Investigation, Formal analysis, Data curation. **Kim Yunsang:** Writing – review & editing, Writing – original draft, Visualization, Validation, Supervision, Resources, Project administration, Methodology, Investigation, Funding acquisition, Formal analysis, Conceptualization. **Sedhain Ganesh:** Writing – original draft,

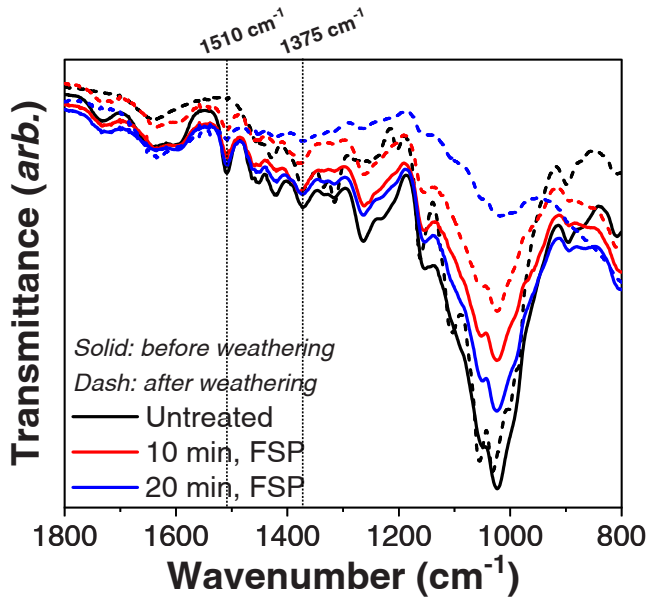

Fig. 9. FTIR spectra of untreated and TiO_2-treated CLT samples (10 and 20 min FSP deposition times) before and after accelerated weathering test.

Table 2
The transmittance ratio of lignin to carbohydrate, I_{lig}/I_{carb}, before and after accelerated weathering test.

Sample description	Transmittance ratio of lignin to carbohydrate, I_{lig}/I_{carb}	Change in I_{lig}/I_{carb} after weathering
Untreated, before weathering	1.05	8.2%
Untreated, after weathering	1.14	
10 min FSP, before weathering	1.04	-0.5%
10 min FSP, after weathering	1.04	
20 min FSP, before weathering	1.03	-3.1%
20 min FSP, after weathering	1.00	

Visualization, Software, Methodology, Investigation, Formal analysis, Data curation.

Declaration of Competing Interest

The authors declare that they have no known competing financial interests or personal relationships that could have appeared to influence the work reported in this paper.

Data Availability

Data will be made available on request.

Acknowledgments

This research was conducted in cooperation with the USDA Forest Service with an award number 20-JV-11111134–036. The authors wish to acknowledge the support of U.S. Department of Agriculture (USDA), Research, Education, and Economics (REE), Agriculture Research Service (ARS), Administrative and Financial Management (AFM), Financial Management and Accounting Division (FMAD) Grants and Agreements Management Branch (GAMB), under Agreement No. 58-0204-9-164. Any opinions, findings, conclusion, or recommendations expressed in this publication are those of the author(s) and do not necessarily reflect the view of the U.S. Department of Agriculture. This publication is a contribution of the Forest and Wildlife Research Center, Mississippi State University. The authors wish to thank Dr. C. Elizabeth Stokes, Amy Rowlen, and Dr. Gabrielly Bobadilha in the Department of Sustainable Bioproducts at Mississippi State University for allowing the use of CLT blocks, accelerated weathering chamber, color spectrophotometer, and glossmeter.

References

[1] G. Wimmers, Wood: a construction material for tall buildings, Nat. Rev. Mater. *2* (12) (2017) 17051.
[2] S. Ayanleye, K. Udele, V. Nasir, X. Zhang, H. Militz, Durability and protection of mass timber structures: a review, J. Build. Eng. *46* (2022) 103731.
[3] M. Kropat, M.A. Hubbe, F. Laleicke, Natural, accelerated, and simulated weathering of wood: a review, BioResources *15* (4) (2020) 9998–10062.
[4] R. Ross, Wood handbook: Wood as an engineering material, Chapter 16 - Finishing Wood. *FPL-GTR 282*2021) 1–543.
[5] W.C. Feist, D.N.S. Hon, Chemistry of Weathering and Protection, in: The Chemistry of Solid Wood, Vol. 207, American Chemical Society, 1984, pp. 401–451.
[6] V. Jirouš-Rajković, J. Miklečić, Enhancing weathering resistance of wood—a review, Polymers *13* (12) (2021) 1980.
[7] B. George, E. Suttie, A. Merlin, X. Deglise, Photodegradation and photostabilisation of wood – the state of the art, Polym. Degrad. Stab. *88* (2) (2005) 268–274.
[8] P. Evans, J. Haase, A. Seman, M. Kiguchi, The search for durable exterior clear coatings for wood, Coatings *5* (4) (2015) 830–864.
[9] L. Wallenhorst, L. Gurău, A. Gellerich, H. Militz, G. Ohms, W. Viöl, UV-blocking properties of Zn/ZnO coatings on wood deposited by cold plasma spraying at atmospheric pressure, Appl. Surf. Sci. *434* (2018) 1183–1192.
[10] G. Jnido, G. Ohms, W. Viöl, Deposition of TiO2 thin films on wood substrate by an air atmospheric pressure plasma jet, Coatings *9* (7) (2019) 441.
[11] P.D. Evans, Review of the weathering and photostability of modified wood, Wood Mater. Sci. Eng. *4* (1-2) (2009) 2–13.
[12] C.U. Pittman, M.G. Kim, D.D. Nicholas, L. Wang, F.R.A. Kabir, T.P. Schultz, L. L. Ingram, Wood enhancement treatments I. Impregnation of southern yellow pine with melamine-formaldehyde and melamine-ammeline-formaldehyde resins, J. Wood Chem. Technol. *14* (4) (1994) 577–603.
[13] L. Kong, H. Guan, X. Wang, In situ polymerization of furfuryl alcohol with ammonium dihydrogen phosphate in poplar wood for improved dimensional stability and flame retardancy, *ACS Sustain. Chem. Eng. 6* (3) (2018) 3349–3357.
[14] C. Hill, M. Altgen, L. Rautkari, Thermal modification of wood—a review: chemical changes and hygroscopicity, J. Mater. Sci. *56* (11) (2021) 6581–6614.
[15] L. Jasmani, R. Rusli, T. Khadiran, R. Jalil, S. Adnan, Application of nanotechnology in wood-based products industry: a review, Nanoscale Res. Lett. *15* (1) (2020) 207.
[16] M. Nikolic, J.M. Lawther, A.R. Sanadi, Use of nanofillers in wood coatings: a scientific review, J. Coat. Technol. Res. *12* (3) (2015) 445–461.
[17] F. Aloui, A. Ahajji, Y. Irmouli, B. George, B. Charrier, Merlin, A., Inorganic UV absorbers for the photostabilisation of wood-clearcoating systems: comparison with organic UV absorbers, Appl. Surf. Sci. *253* (8) (2007) 3737–3745.
[18] M. Vlad Cristea, B. Riedl, P. Blanchet, Enhancing the performance of exterior waterborne coatings for wood by inorganic nanosized UV absorbers, Prog. Org. Coat. Technol. *69* (4) (2010) 432–441.
[19] T. Yi, J.J. Morrell, Role of α-Fe2O3 nano-particles in protecting wood from ultraviolet light degradation, Holzforschung *77* (6) (2023) 453–467.
[20] Y. Wang, X. Wu, Y. Wang, Y. Tian, H. Mu, J. Li, Hydrophobic and UV-resistant properties of environmentally friendly nano-ZnO-coated wood, Holzforschung *75* (2) (2021) 138–147.
[21] H. Guo, D. Klose, Y. Hou, G. Jeschke, I. Burgert, Highly efficient UV protection of the biomaterial wood by a transparent TiO 2 /Ce Xerogel, *ACS Appl. Mater. Interfaces 9* (44) (2017) 39040–39047.
[22] X. Wang, S. Liu, H. Chang, J. Liu, Sol-gel deposition of TiO2 nanocoatings on wood surfaces with enhanced hydrophobicity and photostability, Wood and Fiber Sci. (2014) 109–117.
[23] Y. Fu, W. Fu, Y. Liu, G. Zhang, Y. Liu, H. Yu, Comparison of ZnO nanorod array coatings on wood and their UV prevention effects obtained by microwave-assisted hydrothermal and conventional hydrothermal synthesis, Holzforschung *69* (8) (2015) 1009–1014.
[24] P. Pori, A. Vilčnik, M. Petrič, A. Sever Škapin, M. Mihelčič, A. Šurca Vuk, U. Novak, B. Orel, Structural studies of TiO2/wood coatings prepared by hydrothermal deposition of rutile particles from TiCl4 aqueous solutions on spruce (Picea abies) wood, Appl. Surf. Sci. *372* (2016) 125–138.
[25] S. Kurzinski, P. Crovella, P. Kremer, Overview of Cross-Laminated Timber (CLT) and Timber Structure Standards Across the World, JMass Timber Constr. J. *5* (1) (2022) 1–13.
[26] ltd, R.; Markets, Cross-Laminated Timber Market: Global Industry Trends, Share, Size, Growth, Opportunity and Forecast 2023-2028.
[27] *CLT handbook: cross-laminated timber*. U.S. edition ed.; FPInnovations: Pointe-Claire, QC, 2013.
[28] W.Y. Teoh, R. Amal, L. Mädler, Flame spray pyrolysis: an enabling technology for nanoparticles design and fabrication, Nanoscale *2* (8) (2010) 1324.
[29] H. Teisala, M. Tuominen, M. Aromaa, J.M. Mäkelä, M. Stepien, J.J. Saarinen, M. Toivakka, J. Kuusipalo, Development of superhydrophobic coating on

paperboard surface using the liquid flame spray, Surf. Coat. Technol. *205* (2) (2010) 436–445.
[30] H. Teisala, M. Tuominen, M. Stepien, J. Haapanen, J.M. Mákelá, J.J. Saarinen, M. Toivakka, J. Kuusipalo, Wettability conversion on the liquid flame spray generated superhydrophobic TiO2 nanoparticle coating on paper and board by photocatalytic decomposition of spontaneously accumulated carbonaceous overlayer, Cellulose *20* (1) (2013) 391–408.
[31] G. Sedhain, Modification of wood by liquid-precursor thermal spray coating, Theses and Dissertations (2020) 3167. ⟨https://scholarsjunction.msstate.edu/td/3167⟩.
[32] ASTM Standard G154-16 Practice for Operating Fluorescent Ultraviolet (UV) Lamp Apparatus for Exposure of Nonmetallic Materials. ASTM International.
[33] ISO/CIE 11664-4:2019(en), Colorimetry — Part 4: CIE 1976 L*a*b* colour space.
[34] ISO 2813:2014(en), Paints and varnishes — Determination of gloss value at 20 degrees, 60 degrees and 85 degrees.
[35] G. d S. Bobadilha, C.E. Stokes, K.M. Ohno, G. Kirker, D.J.V. Lopes, M. Nejad, Physical, optical, and visual performance of coated cross-laminated timber during natural and artificial weathering, Coatings *11* (2) (2021) 252.
[36] B. Bhushan, Y.C. Jung, Natural and biomimetic artificial surfaces for superhydrophobicity, self-cleaning, low adhesion, and drag reduction, Prog. Mater Sci. *56* (1) (2011) 1–108.
[37] A.B.D. Cassie, S. Baxter, Wettability of porous surfaces, Trans. Faraday Society *40* (1944) 546.
[38] M.B. Hugenschmidt, L. Gamble, C.T. Campbell, The interaction of H2O with a TiO2 (110) surface, Surf. Sci. *302* (3) (1994) 329–340.
[39] R. Wang, K. Hashimoto, A. Fujishima, M. Chikuni, E. Kojima, A. Kitamura, M. Shimohigoshi, T. Watanabe, Light-induced amphiphilic surfaces, Nature *388* (6641) (1997) 431–432.
[40] R. Wang, K. Hashimoto, A. Fujishima, M. Chikuni, E. Kojima, A. Kitamura, M. Shimohigoshi, T. Watanabe, Photogeneration of highly amphiphilic TiO2 surfaces, Adv. Mater. *10* (2) (1998) 135–138.
[41] Q.F. Xu, Y. Liu, F.-J. Lin, B. Mondal, A.M. Lyons, Superhydrophobic TiO2–Polymer Nanocomposite Surface with UV-Induced Reversible Wettability and Self-Cleaning Properties, *ACS Appl. Mater. Interfaces 5* (18) (2013) 8915–8924.
[42] Z. RongBo, M.A. Tshabalala, L. QingYu, W. HongYan, Weathering performance of wood coated with a combination of alkoxysilanes and rutile TiO2 hierarchical nanostructures, BioResources *10* (4) (2015) 7053-7064.
[43] C.-A. Teacă, D. Roşu, R. Bodîrlău, L. Roşu, Structural changes in wood under artificial UV light irradiation determined by ftir spectroscopy and color measurements – a brief review, BioResources *8* (1) (2013) 1478-1507.
[44] G. Jnido, G. Ohms, W. Viöl, One-step deposition of polyester/TiO2 coatings by atmospheric pressure plasma jet on wood surfaces for UV and moisture protection, Coatings *10* (2) (2020) 184.
[45] A. Pereira Acosta, P. Zanatta, E. Gallio, N. Freire, M. Lazarotto, P.L. Gomes Jardim, D.A. Gatto, M.L. Moreira, A. Pereira Acosta, P. Zanatta, E. Gallio, N. Freire, M. Lazarotto, P.L. Gomes Jardim, D.A. Gatto, M.L. Moreira, Tio2-modified Pinus elliottii: a pine wood presenting increased resistance to water and ultraviolet radiation, Maderas. Ciencia y tecnología *23* (2021).
[46] E.J. Foster, R.J. Moon, U.P. Agarwal, M.J. Bortner, J. Bras, S. Camarero-Espinosa, K.J. Chan, M.J.D. Clift, E.D. Cranston, S.J. Eichhorn, D.M. Fox, W.Y. Hamad, L. Heux, B. Jean, M. Korey, W. Nieh, K.J. Ong, M.S. Reid, S. Renneckar, R. Roberts, J.A. Shatkin, J. Simonsen, K. Stinson-Bagby, N. Wanasekara, J. Youngblood, Current characterization methods for cellulose nanomaterials, Chem. Soc. Rev. *47* (8) (2018) 2609–2679.
[47] P. Nzokou, D.P. Kamdem, Influence of wood extractives on the photo-discoloration of wood surfaces exposed to artificial weathering, Color Res. Appl. *31* (5) (2006) 425–434.
[48] X. Huang, D. Kocaefe, Y. Kocaefe, Y. Boluk, A. Pichette, A spectrocolorimetric and chemical study on color modification of heat-treated wood during artificial weathering, Appl. Surf. Sci. *258* (14) (2012) 5360–5369.
[49] Q. Sun, Y. Lu, H. Zhang, H. Zhao, H. Yu, J. Xu, Y. Fu, D. Yang, Y. Liu, Hydrothermal fabrication of rutile TiO2 submicrospheres on wood surface: An efficient method to prepare UV-protective wood, Mater. Chem. Phys. *133* (1) (2012) 253–258.
[50] P. Fei, H. Xiong, J. Cai, C. Liu, D. Zia ud, Y. Yu, Enhanced the weatherability of bamboo fiber-based outdoor building decoration materials by rutile nano-TiO2, Constr. Build. Mater. *114* (2016) 307–316.
[51] H. Shen, S. Zhang, J. Cao, J. Jiang, W. Wang, Improving anti-weathering performance of thermally modified wood by TiO2 sol or/and paraffin emulsion, Constr. Build. Mater. *169* (2018) 372–378.
[52] *Wood and cellulosic chemistry*, *Chapter 9* - Color and Discoloration. 2nd ed.; Marcel Dekker: New York, 2001; p 914.
[53] M. Mahy, L. Van Eycken, A. Oosterlinck, Evaluation of uniform color spaces developed after the adoption of CIELAB and CIELUV, *Color Res. Appl. 19* (2) (1994) 105–121.
[54] U. Müller, M. Rätzsch, M. Schwanninger, M. Steiner, H. Zöbl, Yellowing and IR-changes of spruce wood as result of UV-irradiation, J. Photochem. Photobiol. B: Biol *69* (2) (2003) 97–105.
[55] K.K. Pandey, Study of the effect of photo-irradiation on the surface chemistry of wood, Polym. Degrad. Stab. *90* (1) (2005) 9–20.
[56] M. Kymäläinen, T.V. Lourençon, K. Lillqvist, Natural weathering of soft- and hardwoods modified by contact and flame charring methods, Eur. J. Wood Wood Prod. *80* (6) (2022) 1309–1320.
[57] T. Yi, J.J. Morrell, Role of α/γ Fe2O3 and ZnO nano-particles in reducing photodegradation of wood components, Wood Sci. Technol. *57* (2) (2023) 427–446.